



# HHS Public Access

Author manuscript

*Nat Biotechnol.* Author manuscript; available in PMC 2013 October 01.

Published in final edited form as:

*Nat Biotechnol.* 2013 April ; 31(4): 335–341. doi:10.1038/nbt.2509.

## Compartmentalization of metabolic pathways in yeast mitochondria improves production of branched chain alcohols

José L. Avalos<sup>1,2</sup>, Gerald R. Fink<sup>2,\*</sup>, and Gregory Stephanopoulos<sup>1,\*</sup>

<sup>1</sup>Department of Chemical Engineering, Massachusetts Institute of Technology, Room 56-469, Cambridge, MA 02139, USA

<sup>2</sup>Whitehead Institute for Biomedical Research, 9 Cambridge Center, Cambridge, MA 02142, USA

### Abstract

Efforts to improve the production of a compound of interest in *Saccharomyces cerevisiae* have mainly involved engineering or overexpression of cytoplasmic enzymes. We show that targeted expression of metabolic pathways to mitochondria can increase production levels compared with expression of the same pathways in the cytoplasm. Compartmentalisation of the Ehrlich pathway into mitochondria increased isobutanol production by 260%, whereas overexpression of the same pathway in the cytoplasm only improved yields by 10%, compared with a strain overexpressing only the first three steps of the biosynthetic pathway. Subcellular fractionation of engineered strains reveals that targeting the enzymes of the Ehrlich pathway to the mitochondria achieves higher local enzyme concentrations. Other benefits of compartmentalization may include increased availability of intermediates, removing the need to transport intermediates out of the mitochondrion, and reducing the loss of intermediates to competing pathways.

### Introduction

Metabolic engineering of cytoplasmic biosynthetic pathways to create industrial strains of *S. cerevisiae* is commonplace, whereas engineering of biosynthetic pathways that function in mitochondria has largely been ignored. Yet, mitochondria have many potential advantages for metabolic engineering, including the sequestration of diverse metabolites, such as heme, tetrahydrofolate, ubiquinone,  $\alpha$ -ketoacids, steroids, aminolevulinic acid, biotin, and lipoic acid<sup>1-15</sup>. In addition, mitochondria contain intermediates of many central metabolic pathways, including the tricarboxylic acid (TCA) cycle, amino acid biosynthesis and fatty acid metabolism<sup>3,8,16,17</sup>.

Users may view, print, copy, download and text and data- mine the content in such documents, for the purposes of academic research, subject always to the full Conditions of use: [http://www.nature.com/authors/editorial\\_policies/license.html#terms](http://www.nature.com/authors/editorial_policies/license.html#terms)

\*To whom correspondence should be addressed: Prof. Gerald R. Fink, Whitehead Institute for Biomedical Research, 9 Cambridge Center, Room 561, Cambridge, MA 02142, USA. [gink@wi.mit.edu](mailto:gink@wi.mit.edu), Ph.: (617) 258-5214, FAX: (617) 258-9872; Prof. Gregory Stephanopoulos, Massachusetts Institute of Technology, Chemical Engineering Department, 77 Massachusetts Avenue, Room 56-469, Cambridge, MA 02139, USA. [gregstep@mit.edu](mailto:gregstep@mit.edu), Ph.: (617) 258-0398, FAX: (617) 258-6876.

**Editors summary:** Relocation of metabolic pathways to yeast mitochondria can increase production levels compared with expression of the same pathways in the cytoplasm.

**Author Contributions:** J.L.A., G.R.F. and G.S. conceived the project, designed the experiments, analyzed the results and wrote the manuscript. J.L.A. designed and made the pJLA vectors, constructed all pathways and strains, and executed all the experiments.

**Competing Financial Interests Statement:** The authors declare no competing financial interests.

The environment within the mitochondrial matrix differs from the cytoplasm, including higher pH, lower oxygen concentration, and a more reducing redox potential<sup>18-20</sup>. This environment may more closely match the optimal for maximal activity of many enzymes such as the iron-sulfur clusters (ISC), which are essential cofactors of enzymes in diverse pathways including branched chain amino acid and isoprenoid biosynthetic pathways, and which are synthesized exclusively in mitochondria<sup>21</sup>. Although ISCs can be exported to the cytoplasm, the molecular machinery that loads ISCs onto extramitochondrial enzymes is likely to be incompatible with most exogenous ISC-apoenzymes, especially those of bacterial, or archaeal origin<sup>22,23</sup>. The smaller volume of mitochondria, could concentrate substrates favoring faster reaction rates and productivity and confine metabolic intermediates avoiding repressive regulatory responses, diversion of intermediates into competing pathways or even toxic effects of intermediates to cytoplasmic or nuclear processes.

To take advantage of the potential attributes of the mitochondrial environment, we engineered yeast mitochondria to produce three advanced biofuels, namely isobutanol, isopentanol and 2-methyl-1-butanol (collectively called fusel alcohols). Isobutanol is synthesized in yeast by the valine Ehrlich degradation pathway<sup>24</sup>, but can also be produced from pyruvate in a biosynthetic pathway that recruits the upstream pathway of valine biosynthesis (Fig. 1). The upstream isobutanol pathway, between pyruvate and  $\alpha$ -ketoisovalerate ( $\alpha$ -KIV), comprises acetolactate synthase (ALS, *ILV2*), ketolacid reductoisomerase (KARI, *ILV5*) and dehydroxyacid dehydratase (DADH, *ILV3*), (Fig. 1). The downstream isobutanol pathway comprises  $\alpha$ -ketoacid decarboxylase ( $\alpha$ -KDC) and alcohol dehydrogenase (ADH).

The complete biosynthetic pathway for isobutanol production has been engineered in bacteria<sup>25-30</sup>. In yeast, the isobutanol biosynthetic pathway is complicated by subcellular compartmentalization: the upstream part of the pathway is confined to mitochondria<sup>3</sup>, whereas the downstream part of the pathway is confined to the cytoplasm (Ehrlich pathway<sup>24</sup>) (Fig. 1A). Therefore the simple overexpression of all the enzymes in the isobutanol pathway could create a significant bottleneck in which the transport of intermediates across membranes reduces productivity and enables these intermediates to be consumed by competing pathways. Nevertheless, the isobutanol pathway has been partially constructed in yeast, by overexpressing only some of the enzymes, and in their natural compartments, to increase isobutanol production<sup>31-33</sup>. Although efforts have been made to transfer the isobutanol pathway, partly or completely, to either compartment<sup>34</sup> (upstream to cytoplasm<sup>35,36</sup>, or downstream to mitochondria<sup>37,38</sup>), there has been no direct comparison of the effects of mitochondrial versus cytoplasmic engineering of downstream enzymes in fully assembled pathways.

Yeast mitochondria have been exploited through gene targeting to produce hydrocortisone<sup>39</sup> and plant terpenoids<sup>40</sup>; however, these pathways were split across multiple subcellular compartments. In this study we engineer strains with complete isobutanol pathways overexpressed in mitochondria to avoid pathway sub-compartmentalization (Fig. 1B), and compare their fusel alcohol production levels with those of strains in which all enzymes of the isobutanol pathway are overexpressed in their

natural compartments (divided into an upstream mitochondrial and downstream cytoplasmic pathways; Fig. 1A). We show that moving the complete pathway into a single compartment (mitochondria) results in a substantial increase in the production of fusel alcohols, and provide evidence that this increase is at least partly due to a higher availability of the key  $\alpha$ -KIV intermediate, and increased local enzyme concentrations due to mitochondrial compartmentalization.

To reconstruct multiple isoforms of the isobutanol pathway we developed a standard, flexible set of vectors (pJLA vector series) that facilitates targeting of identical pathways to either the cytoplasm or mitochondria. These new tools enabled rapid assembly and comparison of eighteen isoforms (or “isopathways”) of the complete isobutanol pathway, in which their downstream enzymes are targeted to either the mitochondria or the cytoplasm, but are in every other way identical. This approach enabled us to measure the effect of mitochondrial engineering of isobutanol pathways for the production of isobutanol, isopentanol and 2-methyl-1-butanol.

## Results

### Construction of partial and complete isobutanol pathways

The enzymes required for the synthesis of isobutanol were cloned using a standardized vector series (pJLA vectors) that we developed for gene overexpression in *S. cerevisiae* (see online Methods). This tool facilitated the assembly of multiple isobutanol isopathways, into single high copy (2 $\mu$ ) plasmids, such that each isopathway was introduced into yeast on a single vector.

The downstream enzymes were targeted to either the cytoplasm or mitochondria (Fig 1), using the N-terminal mitochondrial localization signal (MLS) from subunit IV of the yeast cytochrome c oxidase (CoxIV)<sup>41</sup> (Supplementary Tables 1 and 2). The parallel assembly of cytoplasmic and mitochondrial pathways using pJLA vectors allows for the overexpression of pathways and enzymes that are identical except for the subcellular compartment to which these enzymes are targeted (aside from a single N-terminal glutamine in enzymes targeted to mitochondria<sup>41</sup>).

We prepared multigenic plasmids containing partial or complete isobutanol pathways (Supplementary Tables 1 and 2), each with the same upstream pathway composed of the endogenous *ILV2*, *ILV3* and *ILV5* (*ILV* genes), driven by the *TDH3*, *PGK1*, and *TEF1* promoters respectively. Partial isobutanol pathways were constructed by adding to the upstream pathway construct one of three possible  $\alpha$ -KDCs (LIKivd from *L. lactis*, *KIDI* or *ARO10*, both from *S. cerevisiae*) driven by the *TDH3* promoter and targeted to mitochondria. Complete isobutanol pathway constructs contained, in addition to the upstream pathway, one of the three  $\alpha$ -KDCs driven by the *TDH3* promoter, and one of three possible ADHs (*ADH7* from *S. cerevisiae*, EcFucO from *E. coli*, or LIAdhA<sup>RE1</sup> from *L. lactis*<sup>26</sup>) driven by the *TEF1* promoter; with both downstream enzymes targeted to either mitochondria or the cytoplasm. This assembly produced a total of 4 partial and 18 complete isobutanol pathway constructs (see online Methods and Supplementary Information for details).

## Expression of the isobutanol pathway

Plasmids with partial or complete isobutanol pathways were transformed into yeast (Supplementary Table 3) and the transformants were analyzed for isobutanol production. The average isobutanol titers obtained in 24-hour-long high cell-density fermentations in minimal medium from the various isobutanol isopathways (see online Methods) were compared (Fig. 2A). The increased isobutanol titers are a reflection of increased isobutanol productivity per yeast cell (specific titers), (Fig. 2B), and reproducible (strains had stable productive phenotypes after being stored at 4°C or -80°C, with  $n \geq 3$ ).

The incremental addition of each component of the isobutanol pathway results in cumulative increases in isobutanol production in high cell-density fermentations, but only if the downstream enzymes are targeted to mitochondria (Fig. 2A and B), suggesting that these downstream enzymes are active in mitochondria. The background isobutanol production of yeast transformed with an empty plasmid (JAY2) in 24-hour high cell density fermentations in minimal medium is  $28 \pm 2$  mg/L. When the upstream *ILV* genes are overexpressed (JAY38), isobutanol production increases approximately 5-fold, to  $136 \pm 23$  mg/L. The additional overexpression of the first downstream enzyme ( $\alpha$ -KDC), targeted to mitochondria in strains JAY49, JAY51 and JAY53, resulted in isobutanol titers as high as  $244 \pm 13$  mg/L in JAY51, almost double the production from overexpression of the *ILV* genes alone (JAY38). The overexpression of the complete mitochondrial isobutanol pathway (by adding ADHs targeted to mitochondria in strains JAY153 to JAY161) resulted in isobutanol titers as high as  $486 \pm 36$  mg/L and  $491 \pm 29$  mg/L in JAY153 and JAY161 respectively, which is a further 2-fold increase from the 4-gene isobutanol pathway and almost 18-fold increase from JAY2 (the control strain harboring an empty plasmid). By contrast, yeast overexpressing the downstream  $\alpha$ -KDCs and ADHs targeted to the cytoplasm (strains JAY166 to JAY174) produced isobutanol titers of only  $151 \pm 34$  mg/L in JAY166, similar to the titers produced by JAY38, which overexpresses only the upstream *ILV* genes in mitochondria-(Fig. 2A and B).

The superiority of mitochondrial isobutanol production compared with cytoplasmic isobutanol production was also replicated in fermentations initiated at low cell densities (0.03 OD) both in minimal (Fig. 2C) and complete media (Supplementary Table 4), (see online Methods). The strains expressing mitochondrially-targeted isobutanol downstream pathways, JAY153 and JAY161, outperformed JAY166 and JAY174 in which the same genes were expressed in the cytoplasm, with isobutanol titers as high as  $279 \pm 16$  and  $635 \pm 23$  mg/L in minimal and complete media respectively. Strains JAY166 and JAY174, which overexpress isobutanol downstream pathways in the cytoplasm, achieved titers similar to those obtained with JAY38 (overexpressing only the *ILV* genes in mitochondria), which reached  $157 \pm 12$  mg/L of isobutanol in minimal medium, and  $384 \pm 15$  mg/L in complete medium. By contrast, strain JAY2 (with empty plasmid) produced only  $28 \pm 1$  and  $67 \pm 10$  mg/L of isobutanol in minimal and complete media, respectively (Fig. 2C and Supplementary Table 4).

To determine whether increased availability of  $\alpha$ -KIV in mitochondria has a substantial role in improving the performance of those pathways that were targeted to the mitochondria, we

tested whether increasing the cytoplasmic availability of  $\alpha$ -KIV, by adding this intermediate to the culture media, has an effect on cytoplasmic isobutanol production. Increased availability of  $\alpha$ -KIV in the cytoplasm does increase isobutanol production of strains overexpressing  $\alpha$ -KDCs in the cytoplasm (Fig. 3a), achieving titers that approach those obtained with strains engineered with mitochondrial isobutanol pathways (Fig. 3b). This indicates that  $\alpha$ -KIV is normally a limiting intermediate in the cytoplasm, and that downstream enzymes targeted to mitochondria likely benefit from an increased availability of  $\alpha$ -KIV in this organelle.

### Mitochondrial isobutanol pathways produce other desirable branched alcohols

Yeast strains with mitochondrial isobutanol pathways also produce substantial amounts of isopentanol (3-methyl-1-butanol) and 2-methyl-1-butanol production, compared with strains overexpressing complete isobutanol pathways but with cytoplasmic downstream enzymes. The average isopentanol and 2-methyl-1-butanol titers in 24 hour-long high cell-density fermentations of the different isobutanol constructs show a pattern similar to the one observed in isobutanol production (Fig. 4A and B). In fermentations initiated at low cell densities, overexpressing the *ILV* genes alone (JAY38) or with cytoplasmic downstream pathways (JAY166 and JAY174) has little to no measurable effect on isopentanol and 2-methyl-1-butanol production. However, measurable increases in the production of both alcohols were achieved when complete isobutanol pathways were overexpressed in mitochondria (Supplementary Table 4).

Overexpression of the *ILV* genes alone (JAY38) in high cell-density fermentations results in modest increases in isopentanol ( $28 \pm 5$  mg/L) and 2-methyl-1-butanol ( $19 \pm 8$  mg/L) production, compared with JAY2, which harbors an empty plasmid ( $16 \pm 4$  mg/L and  $11 \pm 1$  mg/L, respectively. Fig. 4a and b). The addition of plasmids harboring  $\alpha$ -KDCs targeted to mitochondria further increased the production of these alcohols to as much as  $65 \pm 17$  mg/L of isopentanol in JAY49, and  $57 \pm 9$  mg/L of 2-methyl-1-butanol in JAY51. Furthermore, when both,  $\alpha$ -KDCs and ADHs are targeted to mitochondria, we obtained titers as high as  $130 \pm 21$  mg/L and  $113 \pm 5$  mg/L of isopentanol and 2-methyl-1-butanol in JAY153 and JAY161 respectively, which represent approximately 8- and 11-fold increases from empty plasmid respectively. In contrast, pathways with the same downstream enzymes targeted to cytoplasm produced only  $28 \pm 5$  mg/L of isopentanol (JAY166), which is indistinguishable from overexpressing the upstream pathway alone (JAY38); and  $8 \pm 4$  mg/L of 2-methyl-1-butanol (JAY174), which is indistinguishable from background (JAY2), (Fig. 4a and b).

### Higher local concentrations of enzymes targeted to mitochondria

To ensure that the CoxIV mitochondrial localization signal targeted enzymes to mitochondria, we quantified the amount of targeted enzymes in subcellular fractionations of our engineered strains. All enzymes fused to the CoxIV mitochondrial localization signal were detected in the mitochondrial fractions, whereas enzymes lacking the CoxIV signal were only detected in cytoplasmic fractions (Fig. 5). Furthermore, three of the four enzymes analyzed show increased local concentrations in mitochondria, compared to cytoplasm (overexpressed under the same promoter), reaching as much as a four-fold increase in Ll-*adhA*<sup>RE1</sup> concentration when targeted to mitochondria. These results confirm not only that

the CoxIV mitochondrial localization signal is an effective signal to target the enzymes in this study to mitochondria, but also that it is possible to achieve higher local enzyme concentrations through targeting to this organelle, probably owing to the smaller volume of mitochondria compared to the cytoplasm.

## Discussion

Our results show that targeting the entire isobutanol pathway to mitochondria significantly improves its titer, yield and productivity, compared with a partly cytoplasmic equivalent. Isobutanol production is substantially increased when the overexpression of the downstream enzymes ( $\alpha$ -KDC and ADH) is targeted to mitochondria rather than to the cytoplasm. To measure the effect of mitochondrial engineering, we analyzed the isobutanol titers obtained in high cell-density fermentations in minimal media when downstream enzymes, supplementing the overexpression of *ILV* genes, are targeted to either mitochondria or the cytoplasm (Fig. 2a and b). In this manner, JAY153 (with mitochondrial L1-kivd and Sc-adh7) produces  $486 \pm 36$  mg/L of isobutanol, whereas JAY166 (with the same downstream enzymes targeted to cytoplasm) produces  $151 \pm 34$  mg/L. Since JAY38 (which overexpresses only the *ILV* genes) produces  $136 \pm 23$  mg/L of isobutanol, the effect of targeting L1-kivd and Sc-adh7 to mitochondria is approximately a 260% improvement in isobutanol titers, as opposed to a maximum improvement of 10% seen when the same enzymes are targeted to the cytoplasm (JAY166 isobutanol titers are the highest of all strains overexpressing cytoplasmic downstream enzymes). (Fig. 2a and b).

Our combinatorial constructs permitted a rapid comparison of the efficacy of native and heterologous enzymes for isobutanol production. The choice of decarboxylase in the downstream isobutanol pathway produced significant effects, whereas the activity of the three selected dehydrogenases seemed equivalent (Fig. 2a and b). The specific  $\alpha$ -KDC homologue used has an important impact on titers of isobutanol, with L1-kivd and Sc-aro10 being substantially more active than Sc-kid1. By contrast, the three ADHs selected in this study are roughly equally active, despite the reported NADPH dependence of Sc-adh7<sup>42</sup>, the improved affinity for isobutyraldehyde of L1-adhA<sup>RE1</sup><sup>26</sup>, and the ability of Ec-fucO to reduce relatively large aldehydes<sup>43</sup>.

Isopentanol and 2-methyl-1-butanol titers are also increased in strains containing mitochondrial isobutanol pathways. These increased titers are likely owing to: (1) expression of the upstream *ILV* genes (*ILV2*, *ILV3* and *ILV5*), also involved in the biosynthetic pathways of leucine and isoleucine, resulting in the production of the relevant  $\alpha$ -ketoacids ( $\alpha$ -ketoisocaproate and  $\alpha$ -keto-3-methylvalerate, respectively), (Fig. 4C); (2) the two  $\alpha$ -ketoacid precursors to these alcohols being suitable substrates for the overexpressed  $\alpha$ -KDCs, with L1-kivd having a bias for isopentanol production, Sc-aro10 higher activity for 2-methyl-1-butanol production, and Sc-kid1 no detectable activity; and (3) the aldehydes they produce being potential substrates for the three overexpressed ADHs, which have no apparent preference for the production of either alcohol (Fig. 4 and Supplementary Table 4).

In common with isobutanol production, the overexpression of  $\alpha$ -KDCs and ADHs increases the production of isopentanol and 2-methyl-1-butanol but only when these enzymes are targeted to mitochondria. Moreover, the effects of mitochondrial engineering on the production of isopentanol and 2-methyl-1-butanol in high cell-density fermentations are even larger than those observed for isobutanol. Overexpression of downstream enzymes of the isobutanol pathway in mitochondria increased isopentanol and 2-methyl-1-butanol titers (from the overexpression of *ILV* genes alone) by as much as 370% and 500%, respectively. In the case of 2-methyl-1-butanol (as with isobutanol), this is probably due to the fact that its  $\alpha$ -ketoacid precursor,  $\alpha$ -keto-3-methylvalerate, is synthesized in mitochondria, and thus has higher availability in this organelle. However, the case of isopentanol is paradoxical since its  $\alpha$ -ketoacid precursor,  $\alpha$ -ketoisocaproate, is synthesized in the cytoplasm. It is possible that mitochondrial pathways, by consuming  $\alpha$ -ketoisovalerate in mitochondria, mitigate the repression that *ILV* gene overexpression is likely to effect on  $\alpha$ -ketoisocaproate biosynthesis (and thus isopentanol production), due to the tight regulation of leucine biosynthesis<sup>3</sup>.

Mitochondrial engineering offers a more frugal way to direct metabolic flux towards isobutanol production, compared with other possible isobutanol pathway configurations. Pathways in which the downstream enzymes are expressed in the cytoplasm, and separated from the mitochondrial upstream pathway (as in strains JAY166-JAY174) might benefit from the overexpression of branched-chain aminoacid aminotransferases (*BAT1* and *BAT2*, Fig1A), as suggested by the overexpression of cytoplasmic *BAT2*<sup>31</sup>. However, in order to exploit the increased abundance of  $\alpha$ -ketoisovalerate provided by the upstream pathway in this configuration, it would be necessary to overexpress at least one, and most likely two additional genes (*BAT1* and *BAT2*), compared to fully mitochondrial pathways. This not only increases the engineering burden, but also increases the chances of off-target effects, such as the possibility of overproducing valine as a side product. Thus, mitochondrial engineering offers a more efficient way to direct the increased metabolic flux provided by overexpressed *ILV* genes towards isobutanol, without invoking valine as an intermediate.

Expression of the complete isobutanol pathway in the cytoplasm by overexpression of *ILV2*, *ILV3* and *ILV5* simply lacking mitochondrial localization signals does not increase isobutanol production<sup>33,35,36</sup>, because these enzymes themselves are tailored for the mitochondrial environment. Increased isobutanol production in the cytoplasm might be achieved by other means but requires, among other things, extensive modifications of all upstream enzymes (all of heterologous origin), overexpression of native and heterologous iron-sulfur cluster assembly and insertion machineries (to obtain cytosolically active *ILV3* homologues), and overexpression of multiple native and heterologous chaperones<sup>36</sup>. These numerous manipulations contrast with the modest changes required to achieve an approximately 5-fold increase in isobutanol production by overexpressing the native *ILV* genes in their natural environment of mitochondria.

The titers, yields and productivities of isopentanol and 2-methyl-1-butanol we achieved (Table 1) with JAY161, are the highest ever reported. Our isobutanol productivity is more than double than the highest reported in the literature<sup>35</sup>, and our titers are as high as the highest ever reported, but our strains required higher sugar concentrations. Furthermore, our strains produced substantial yields of isobutanol in complete media containing valine,

whereas engineering the complete pathway for overexpression in the cytoplasm rendered it sensitive to inhibition by valine<sup>35</sup>, a nutrient that is likely to be present in industrial feedstocks. While these alcohols are known to be toxic, even our best isobutanol producers did not show any reduced fitness, measured by growth rate or maximal cellular density. The challenge to further improve yields, titers and productivities will require diverting more carbon flux, from ethanol to branched-chain alcohols production<sup>32,44</sup>.

The strategy of organelle targeting has been applied in plants, where portions of the isoprenoid pathway have been targeted to plastids of the tobacco plant<sup>45</sup>. Unlike our study, the pathways compared in tobacco plant cytoplasm (mevalonate pathway) and chloroplast (methylerythritol pathway) were not identical, and only their downstream enzymes were overexpressed. Nevertheless, the targeting of a metabolic pathway to the plant plastid, as with our redirection of the isobutanol pathway to yeast mitochondria, resulted in marked increases in the production levels of the desired end-products. The sequestration of the isoprenoid pathway in plastids, in common with the confinement of the isobutanol pathway to mitochondria in yeast, might benefit from higher concentrations of enzymes, substrates and cofactors, which would favor higher productivities.

We have shown that for isobutanol production in yeast, sequestration of the pathway in the mitochondrion results in higher enzyme concentrations, probably due to their confinement in the relatively smaller volume of the mitochondrial compartment. Moreover, the key  $\alpha$ -KIV intermediate is limiting in the cytosol, but not in mitochondria; thus targeting the full pathway to mitochondria benefits from increased  $\alpha$ -KIV availability, eliminates the bottleneck of exporting  $\alpha$ -KIV to the cytoplasm, and reduces the loss of  $\alpha$ -KIV to competing reactions. Pathways targeted to mitochondria may be further enhanced by mutagenesis.

Pathways that are naturally cytoplasmic might also benefit from mitochondrial compartmentalization, as the confinement of enzymes and metabolites to subcellular compartments may result not only in an increase in their local concentrations and proximities, but also in the ability to reduce the toxicity of pathway intermediates, bypass inhibitory regulatory networks, or avoid competing pathways. Thus, subcellular metabolic engineering has the potential to provide multiple mechanisms to improve the performance of engineered pathways.

## Methods

### pJLA Vectors – New tools for yeast metabolic engineering

The challenges to re-engineering a biosynthetic pathway in yeast include the necessity of cloning the ensemble of enzymes required for the multiple steps in the pathway, overexpressing those enzymes, and, for the benefit of mitochondrial engineering, retaining the option to target enzymes to the mitochondrion. To expedite this process, permit the screening of enzymes and promoters, and facilitate the assembly and troubleshooting of engineered pathways, we developed a new standardized vector series, the pJLA vectors, for gene expression in *S. cerevisiae*, which are applicable to mitochondrial as well as classical metabolic engineering.



The pJLA vectors are derived from the pRS vector series<sup>46</sup>. A key feature in this series is a uniform multicloning sequence (MCS) array flanked by a variety of promoters and terminators; start and stop codons; and optional in-frame tags (Supplementary Figure. 1A). This assembly allows the parallel cloning of genes into any vector of the series to build constructs with different promoters, and the option to produce untagged protein, add an N- or C- terminal affinity tag (his-, HA- or Myc-tags), or the N-terminal mitochondrial localization signal (MLS) of the yeast cytochrome c oxidase, subunit IV, CoxIV.

A second key feature in pJLA vectors is the ability to insert multiple gene expression cassettes into a single plasmid, in tandem or inverted directions, so that an entire metabolic pathway may be introduced into yeast via a single vector (Supplementary Figure 1B). What makes this feasible is a triad of unique restriction sites (XmaI/MreI/AscI) that flank all expression cassettes. This feature allows the sequential insertion of multiple gene expression cassettes into the same plasmid by the iterative ligation of inserts obtained from XmaI/AscI digestions into vectors linearized with MreI/AscI, which produce a tandem insertion, an undigestible XmaI/MreI scar, and a new triad of XmaI/MreI/AscI unique sites, available to repeat the reaction for a subsequent insertion. Similar strategies to assemble multiple pieces of DNA have been applied in the BioBricks system<sup>47</sup>. These pJLA vectors have another very useful feature: double digestion of assembled multigenic plasmids with SacI and AscI results in the excision of one DNA fragment per inserted cassette, whose characteristic restriction pattern is diagnostic (Supplementary Figure 2I).

The various applications of the pJLA vectors were indispensable for the expeditious combinatorial engineering of mitochondrial and partly cytoplasmic isobutanol pathways (Supplementary Figure 2 and Supplementary Table 2). A convenient numerical nomenclature (Supplementary Table 5) permits the rapid identification of the main features contained in each vector (see Supplementary Information for details), and facilitates the naming of vectors derived from future expansions to this series.

### Cloning and screening of isobutanol pathway components

The pJLA vectors permitted assembly of various partial and complete isobutanol pathways, in which the downstream pathway enzymes were targeted to either the mitochondria or the cytoplasm (Fig. 1). Initially gene expression cassettes in pJLA vectors were constructed for each individual enzyme (using three possible constitutive promoters and three possible affinity tags, Supplementary Table 1). The upstream isobutanol pathway was constructed by cloning the yeast endogenous *ILV2*, *ILV3*, and *ILV5* genes in vectors pJLA121<sup>013C3F</sup>, pJLA121<sup>031C1F</sup>, and pJLA121<sup>022C2F</sup>, respectively. These vectors lack the engineered CoxIV mitochondrial localization signal of the pJLA series, as these enzymes are naturally targeted to mitochondria (Fig. 1).

To test multiple enzymes of the downstream isobutanol pathway (Ehrlich, pathway), we first used vectors pJLA121<sup>021C1F</sup> and pJLA121<sup>121C1F</sup>, which fuse a C-terminal his tag to genes driven by a *TEF1* promoter, and target the gene products to the cytoplasm or mitochondrion, respectively. Using these vectors we screened  $\alpha$ -KDCs and ADHs from various organisms to compare the levels of expression in yeast mitochondria and cytoplasm by Western blot (Supplementary Figure. 2A and B). We also evaluated the increase in isobutanol production

obtained with different  $\alpha$ -KDCs overexpressed by themselves, or in combination with the upstream *ILV* genes, and targeted either to the cytoplasm or to mitochondria (data not shown).

### Construction of a complete mitochondrial or partly cytoplasmic isobutanol pathway

The screens above, and the known biochemistry of candidate enzymes, informed the selection of three decarboxylases and three dehydrogenases used to build complete isobutanol pathways. The three  $\alpha$ -KDCs we selected are *KID1*, and *ARO10* from *S. cerevisiae*, both of which have been implicated in the Ehrlich pathway<sup>24</sup>; and *Llkivd* from *L. lactis*, which has been successfully used in several constructions of the isobutanol biosynthetic pathway<sup>48</sup>. Our selections for dehydrogenases are *ADH7* from *S. cerevisiae*, which has also been implicated in fusel alcohol production in yeast<sup>42</sup>; *EcfucO* from *E. coli*, which has been successfully used in the synthesis of heavy alcohols via the reverse beta-oxidation of fatty acids in bacteria<sup>43</sup> and *LladhA<sup>RE1</sup>* from *L. lactis*, which has been engineered for increased affinity for isobutyraldehyde<sup>26</sup>. This set of enzymes was selected in the combinatorial assembly of complete isobutanol isopathways with their downstream components targeted to either mitochondria or cytoplasm.

Using the multigenic assembly tool of pJLA vectors, we prepared constructs containing partial or complete isobutanol pathways. The assembly of complete isobutanol pathways using the six selected downstream enzymes in all possible combinations yielded nine mitochondrial constructs and nine cytoplasmic counterparts (Supplementary Table 2). We also prepared partial pathways containing the three upstream *ILV* genes (*ILV2*, *ILV3* and *ILV5*), either by themselves, or with each of the three selected  $\alpha$ -KDCs targeted to mitochondria.

### Cloning

The cloning required to develop the pJLA vectors and isobutanol pathways was carried out using the DH5 $\alpha$  strain of *E. coli*. Endogenous genes of the isobutanol pathway (*ILV2*, *ILV3*, *ILV5*, *KID1*, *ARO10* and *ADH7*) were amplified with PCR, using primers containing *NheI* and *XhoI* restriction sites, which were used to insert all genes into pJLA vectors. Genes from other organisms were synthesized by Bio Basic inc., with codons optimized for *S. cerevisiae*. These genes were designed with flanking *NheI* and *XhoI* sites at the 5' and 3' ends respectively (used to insert them into pJLA vectors), and avoiding restriction sites for *XmaI*, *MreI*, *AscI* and other relevant restriction enzymes.

Enzymes were purchased from NEB (*SacI*, *NheI*, *XbaI*, *XhoI*, *KpnI*, T4-DNA ligase and Phusion polymerase) or Fermentas (*XmaI*, *AscI*, *BspEI* and *MreI*), and reactions were carried out following manufacturers' instructions.

The quality of all vectors was verified before using them for yeast transformation. First we carried out analytical digests of multigenic vectors using *SacI/AscI* double-digestion, which results in the excision of one DNA fragment per inserted cassette (Supplementary Figure 2I); as well as *XhoI* digestion which cuts the vector once per inserted cassette (not shown).

The vectors that produced the expected restriction patterns were subsequently sequenced by the Koch Institute Biopolymers and Proteomic Facility at MIT.

### Yeast strains and transformations

The parental strain in this work is the product of mating BY4741 with Y3929, to produce JAY1 (Supplementary Table 3). The only auxotrophic marker not complemented by this mating is *ura3 $\Delta$ 0*, which serves as a marker for all vectors used. All yeast transformations for isobutanol production studies were carried out on JAY1, using standard lithium acetate protocols, and the resulting strains are catalogued in Supplementary Table 3. Transformation reactions with plasmids containing partial or complete isobutanol pathways resulted in a highly heterogeneous collection of transformants, displaying a wide variability in colony size, growth rates and fusel alcohol productivities. To identify the transformants with the highest fusel alcohol production capabilities we screened multiple colonies of each transformation in high cell-density fermentations.

### High Cell Density Fermentations

Single colonies were grown over night in synthetic complete medium minus uracil, and 2% glucose, at 30 °C. The next day, 4 mL of each overnight culture were centrifuged at 3000 rpm for 3 minutes, the supernatant discarded, and the cells resuspended in 10 mL of minimal medium (1 $\times$ YNB) with 10% glucose, in sterile 50 mL conical tubes. Cells were grown in this medium for 12 to 20 hr at 30 °C and 350 rpm agitation, after which they were centrifuged again at 3000 rpm for 3 min and resuspended in 10 mL of fresh minimal medium with 20% glucose. Fermentations were kept in semi-aerobic conditions in the same 50 mL conical tubes, at 30 °C and shaking at 350 rpm for 24 hours. The initial and final optical densities at 600 nm were averaged to calculate the specific productivities of the heavy alcohols. Variations to this protocol, in which fermentations were carried out in 15% glucose, instead of 20%, produced the same heavy alcohol titers and productivities in all strains tested.

### Fermentations Initiated at Low Cell Densities

Single colonies were grown overnight in 5 mL of synthetic complete medium, minus uracil, and 2% glucose, at 30 °C. These overnight cultures were used the next day to inoculate 15 mL of minimal (1 $\times$ YNB) or synthetic complete (minus uracil) media with 15% or 10% glucose, to an initial OD of 0.03. These fermentations were carried out in sterile 50 mL conical tubes, shaken at 350 rpm and kept at 30 °C for four days. Samples were taken at 0h, 12h, 1d, 2d, 3d, and 4d to measure their optical densities at 600 nm, as well as concentrations of ethanol, isobutanol, isopentanol and 2-methyl-1-butanol.

### Cytoplasmic isobutanol production from supplemented $\alpha$ -ketoisovalerate

To increase the cytoplasmic availability of  $\alpha$ -ketoisovalerate ( $\alpha$ -KIV), this intermediate was added to the fermentation medium. Cells overexpressing an  $\alpha$ -KDC (LI-kivd) in the cytoplasm were grown over night in SD medium (without uracil) with 2% glucose. These cells were used the following day to inoculate 10 mL of SD medium (without uracil) with

2% glucose, and containing 0, 4 or 8 g/L of  $\alpha$ -KIV (Sigma). Fermentations were carried out in sterile 50 ml conical tubes, shaken at 350 rpm and kept at 30 °C for two days.

### Analysis of heavy alcohols

The concentrations of heavy alcohols and ethanol were quantified with HPLC, using and Agilent 1100 series instrument. Samples were centrifuged and filtered to remove cells and other solid debris, and analyzed using an Aminex HPX-87H ion exchange column from Bio-Rad. The column was eluted with 5mM H<sub>2</sub>SO<sub>4</sub> at 55 °C, and 0.75 ml/min for 42 minutes, which provided adequate separation of all alcohols, including isopentanol from 2-methyl-1-butanol. Alcohols were monitored with a refractive index detector, and their peak areas compared to those of standard alcohol solutions for quantification.

### Protein blotting, immunodetection and quantification

To detect expression of tagged protein in full cells by western blot, we collected 1 mL of cells at OD 10.0, (or its equivalent). Cells were centrifuged for 3 minutes at 3000 rpm and 4 °C, and the pellets resuspended in 1 mL of 5% trichloroacetic acid (TCA) solution. After incubating in ice for 10 minutes, the cells were centrifuged again for 3 minutes at 3000 rpm and 4 °C, and the pellets resuspended in 150  $\mu$ L of 10 mM Tris pH 7.5, 1 mM EDTA, 3 mM DTT. Then 150  $\mu$ L of glass beads were added to each tube, and cells were broken on a fastprep cell disrupter (2 cycles of 45 seconds at 6.5 speed with a 5 minute ice incubation in between). Finally, 75  $\mu$ L of 3 $\times$  SDS sample buffer was added to each sample. Equal amounts of sample were loaded to polyacrylamide gels (typically 5 – 15  $\mu$ L), and standard electrophoresis and protein transfer were used to blot proteins on to PVDF membranes.

For quantitative immunoblotting of subcellular fractions, we isolated the cytoplasmic and mitochondrial fractions of engineered strains, as previously described<sup>49</sup>. We measured the total protein in each subcellular fraction using the Pierce BCA Protein Assay Kit (Thermo Scientific), following manufacturer's instructions, loaded 20  $\mu$ g of total protein of each subcellular fraction to each lane of a polyacrylamide gel, and transferred the proteins to PVDF membranes.

Proteins tagged with his-, Myc- or HA- tags were detected using the antibodies: anti-His6-Peroxidase (Roche), c-Myc (9E10):sc-40 (Santa Cruz Biotechnology) and anti HA-Peroxidase, High Affinity (3F10), (Roche) respectively, following manufacturers' instructions. The anti-His6 antibody was used at a dilution of 1:10,000, the anti-HA was used at 1:100,000, and the anti Myc at 1:1,000. As control for subcellular fractionation experiments, anti yeast PGK (22C5D8, Invitrogen) was used at 1:10,000 dilution, and anti yeast porin (16G9E6BC4, Invitrogen) at 1:20,000 dilution, which are specific markers for the cytoplasmic and mitochondrial fractions, respectively. The secondary antibody for detection of c-Myc, anti-PGK or anti-porin was peroxidase labeled anti-mouse antibody (NA931V, ECL), used at a 1:20,000 dilution. The blots were developed using the SuperSignal West Femto developer kit (Thermo scientific). For quantitative measurements, the BIO RAD Chemi Doc XRS + imaging system and Image Lab 3.0.1 software were used to acquire image data, and the ImageJ software was used to quantify luminescent signals by analytical densitometry.

## Protein purification

Protein purification of some enzymes fused to C-terminally his tags was carried out from cells grown to stationary phase in synthetic complete media lacking uracil, with 15-20% glucose. Cells were lysed using a SPEX freezer-mill, model 6870, and the soluble fraction run through a TALON metal affinity resin column, following manufacturer's instructions.

## Fluorescence microscopy

To validate the mitochondrial targeting capabilities of pJLA vectors, we used fluorescence microscopy of cells expressing GFP in either mitochondrial or cytoplasmic constructs. To compare the localization of GFP with that of mitochondria we used MitoFluor Red 589 (Invitrogen), a red fluorescent dye that specifically stains mitochondria. Cells were incubated in a 1 mM solution of MitoFluor Red 589 at 30 °C for 30 minutes and washed in PBS before imaging.

Fluorescence microscopy was done with an inverted Nikon TE2000-s microscope equipped with a Spot RT Camera from Diagnostic Instruments. Samples were loaded on glass slides and visualized with a 100×/1.30 H/N2 oil immersion objective at room temperature. Green fluorescence (GFP) was monitored at 500nm using a HQ:F blocking filter (Nikon). Red fluorescence (MitoFluor Red 589) was monitored at 594nm with a G-2E/C blocking filter (Nikon). The imaging camera was set to capture 8-bit images that were subsequently processed with Photoshop (Adobe Systems).

## Supplementary Material

Refer to Web version on PubMed Central for supplementary material.

## Acknowledgments

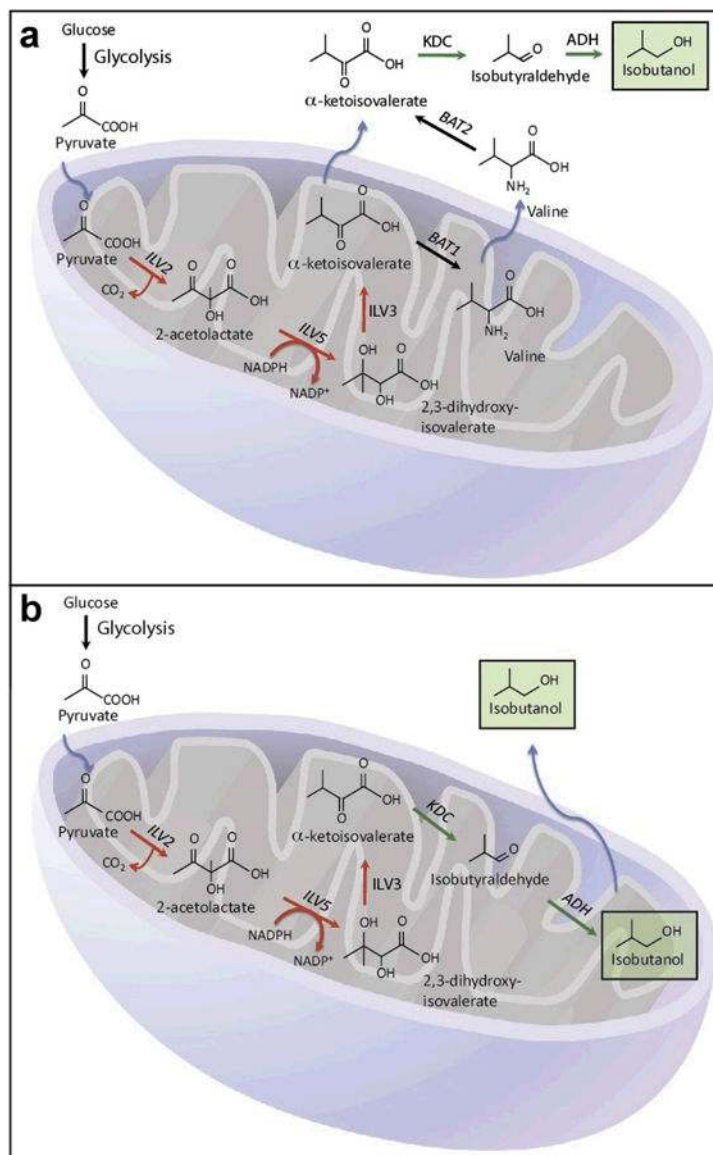
We thank Professors Kristala L. Jones Prather and Thomas D. Fox for helpful discussions, Timothy J. Helbig for working on GFP subcellular localization experiments, Tom DiCesare for preparation of figures, Professor Susan Lindquist for strain Y3929, and members of the Stephanopoulos, Fink, and Prather lab for discussions and advice. J.L.A. is supported by NIH under Ruth L. Kirchstein National Research Service Award 1F32GM098022-01A1. G.R.F. is supported by NIH grant GM040266. This work was supported by Shell Global Solutions (US) Inc.

## References

1. Attardi G, Schatz G. Biogenesis of mitochondria. *Annu Rev Cell Biol.* 1988; 4:289–333. [PubMed: 2461720]
2. Fukuda H, Casas A, Battle A. Aminolevulinic acid: from its unique biological function to its star role in photodynamic therapy. *Int J Biochem Cell Biol.* 2005; 37:272–276. [PubMed: 15474973]
3. Kohlhaw GB. Leucine biosynthesis in fungi: entering metabolism through the back door. *Microbiol Mol Biol Rev.* 2003; 67:1–15. table of contents. [PubMed: 12626680]
4. Kumar A, et al. Subcellular localization of the yeast proteome. *Genes Dev.* 2002; 16:707–719. [PubMed: 11914276]
5. Lange H, Kispal G, Lill R. Mechanism of iron transport to the site of heme synthesis inside yeast mitochondria. *J Biol Chem.* 1999; 274:18989–18996. [PubMed: 10383398]
6. Marquet A, Bui BT, Florentin D. Biosynthesis of biotin and lipoic acid. *Vitam Horm.* 2001; 61:51–101. [PubMed: 11153271]
7. Neuburger M, Rebeille F, Jourdain A, Nakamura S, Douce R. Mitochondria are a major site for folate and thymidylate synthesis in plants. *J Biol Chem.* 1996; 271:9466–9472. [PubMed: 8621617]

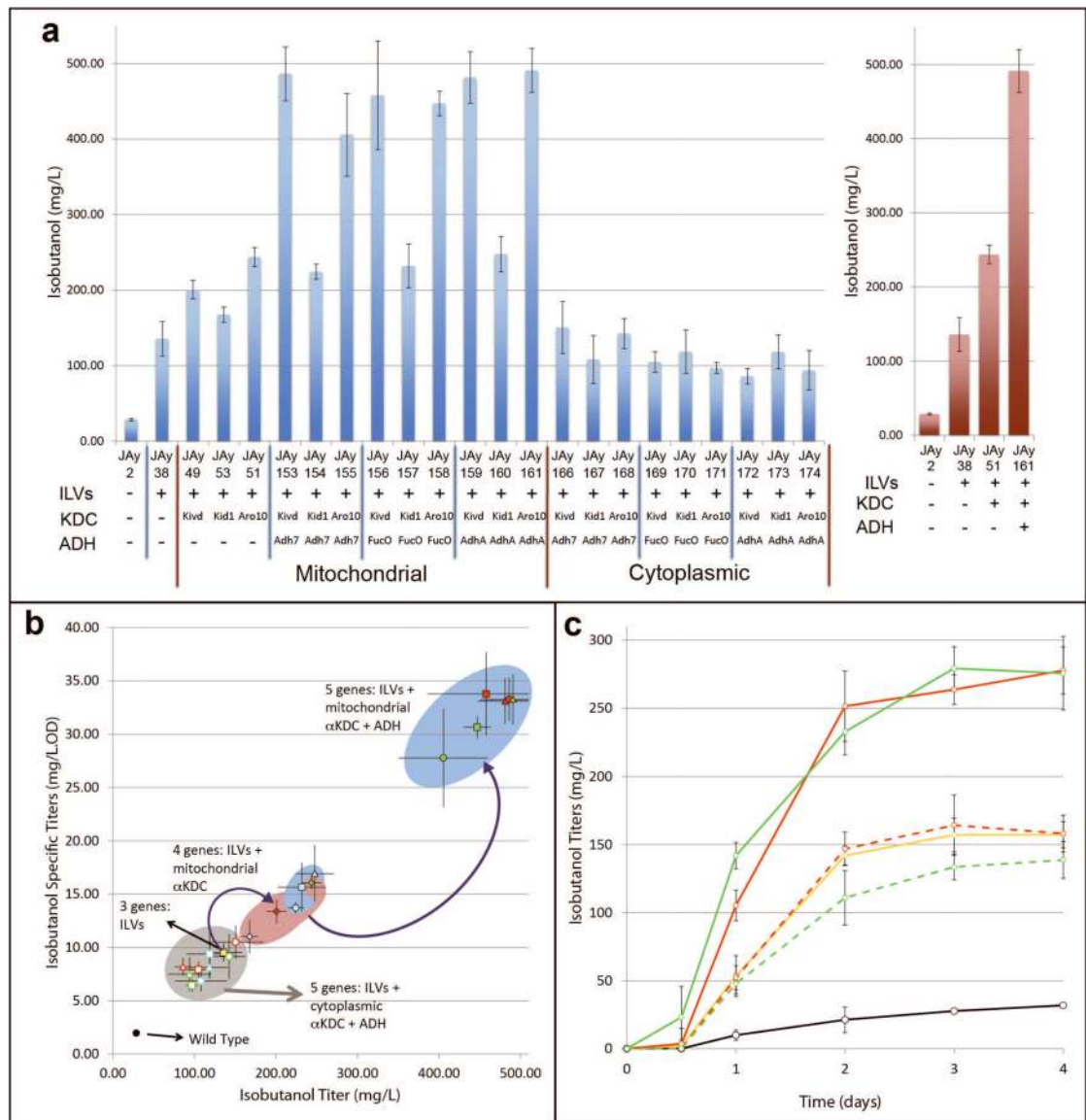
8. Paltauf, F.; Kohlwein, SD.; Henry, SA. *The Molecular and Cellular Biology of the Yeast Saccharomyces*. Jones, EW.; Pringle, JR.; Broach, JR., editors. Cold Spring Harbor Laboratory Press; 1992.
9. Pierrel F, et al. Involvement of mitochondrial ferredoxin and para-aminobenzoic acid in yeast coenzyme Q biosynthesis. *Chem Biol*. 2010; 17:449–459. [PubMed: 20534343]
10. Schonauer MS, Kastaniotis AJ, Kursu VA, Hiltunen JK, Dieckmann CL. Lipoic acid synthesis and attachment in yeast mitochondria. *J Biol Chem*. 2009; 284:23234–23242. [PubMed: 19570983]
11. Shannon KW, Rabinowitz JC. Isolation and characterization of the *Saccharomyces cerevisiae* MIS1 gene encoding mitochondrial C1-tetrahydrofolate synthase. *J Biol Chem*. 1988; 263:7717–7725. [PubMed: 2836393]
12. Sulo P, Martin NC. Isolation and characterization of LIP5. A lipoate biosynthetic locus of *Saccharomyces cerevisiae*. *J Biol Chem*. 1993; 268:17634–17639. [PubMed: 8349643]
13. Tran UC, Clarke CF. Endogenous synthesis of coenzyme Q in eukaryotes. *Mitochondrion*. 2007; 7:S62–71. [PubMed: 17482885]
14. Urban-Grimal D, Volland C, Garnier T, Dehoux P, Labbe-Bois R. The nucleotide sequence of the HEM1 gene and evidence for a precursor form of the mitochondrial 5-aminolevulinate synthase in *Saccharomyces cerevisiae*. *Eur J Biochem*. 1986; 156:511–519. [PubMed: 3516694]
15. Zhang S, Sanyal I, Bulboaca GH, Rich A, Flint DH. The gene for biotin synthase from *Saccharomyces cerevisiae*: cloning, sequencing, and complementation of *Escherichia coli* strains lacking biotin synthase. *Arch Biochem Biophys*. 1994; 309:29–35. [PubMed: 8117110]
16. Hiltunen JK, et al. Mitochondrial fatty acid synthesis type II: more than just fatty acids. *J Biol Chem*. 2009; 284:9011–9015. [PubMed: 19028688]
17. Stryer, L. *Biochemistry*. 4th. W.H. Freeman and Company; 1995.
18. Hu J, Dong L, Outten CE. The redox environment in the mitochondrial intermembrane space is maintained separately from the cytosol and matrix. *J Biol Chem*. 2008; 283:29126–29134. [PubMed: 18708636]
19. Orij R, Postmus J, Ter Beek A, Brul S, Smits GJ. In vivo measurement of cytosolic and mitochondrial pH using a pH-sensitive GFP derivative in *Saccharomyces cerevisiae* reveals a relation between intracellular pH and growth. *Microbiology*. 2009; 155:268–278. [PubMed: 19118367]
20. Schnell N, Krems B, Entian KD. The PAR1 (YAP1/SNQ3) gene of *Saccharomyces cerevisiae*, a c-jun homologue, is involved in oxygen metabolism. *Curr Genet*. 1992; 21:269–273. [PubMed: 1525853]
21. Muhlenhoff U, Lill R. Biogenesis of iron-sulfur proteins in eukaryotes: a novel task of mitochondria that is inherited from bacteria. *Biochim Biophys Acta*. 2000; 1459:370–382. [PubMed: 11004453]
22. Lill R, Muhlenhoff U. Iron-sulfur-protein biogenesis in eukaryotes. *Trends Biochem Sci*. 2005; 30:133–141. [PubMed: 15752985]
23. Xu XM, Moller SG. Iron-sulfur cluster biogenesis systems and their crosstalk. *Chembiochem*. 2008; 9:2355–2362. [PubMed: 18798211]
24. Hazelwood LA, Daran JM, van Maris AJ, Pronk JT, Dickinson JR. The Ehrlich pathway for fusel alcohol production: a century of research on *Saccharomyces cerevisiae* metabolism. *Appl Environ Microbiol*. 2008; 74:2259–2266. [PubMed: 18281432]
25. Atsumi S, Hanai T, Liao JC. Non-fermentative pathways for synthesis of branched-chain higher alcohols as biofuels. *Nature*. 2008; 451:86–89. [PubMed: 18172501]
26. Bastian S, et al. Engineered ketol-acid reductoisomerase and alcohol dehydrogenase enable anaerobic 2-methylpropan-1-ol production at theoretical yield in *Escherichia coli*. *Metab Eng*. 2011; 13:345–352. [PubMed: 21515217]
27. Higashide W, Li Y, Yang Y, Liao JC. Metabolic engineering of *Clostridium cellulolyticum* for production of isobutanol from cellulose. *Appl Environ Microbiol*. 2011; 77:2727–2733. [PubMed: 21378054]
28. Jia X, Li S, Xie S, Wen J. Engineering a Metabolic Pathway for Isobutanol Biosynthesis in *Bacillus subtilis*. *Appl Biochem Biotechnol*. 2011

29. Li S, Wen J, Jia X. Engineering *Bacillus subtilis* for isobutanol production by heterologous Ehrlich pathway construction and the biosynthetic 2-ketoisovalerate precursor pathway overexpression. *Appl Microbiol Biotechnol.* 2011; 91:577–589. [PubMed: 21533914]
30. Smith KM, Cho KM, Liao JC. Engineering *Corynebacterium glutamicum* for isobutanol production. *Appl Microbiol Biotechnol.* 2010; 87:1045–1055. [PubMed: 20376637]
31. Chen X, Nielsen KF, Borodina I, Kielland-Brandt MC, Karhumaa K. Increased isobutanol production in *Saccharomyces cerevisiae* by overexpression of genes in valine metabolism. *Biotechnol Biofuels.* 2011; 4:21. [PubMed: 21798060]
32. Kondo T, et al. Genetic engineering to enhance the Ehrlich pathway and alter carbon flux for increased isobutanol production from glucose by *Saccharomyces cerevisiae*. *J Biotechnol.* 2012; 159:32–37. [PubMed: 22342368]
33. Lee WH, et al. Isobutanol production in engineered *Saccharomyces cerevisiae* by overexpression of 2-ketoisovalerate decarboxylase and valine biosynthetic enzymes. *Bioprocess Biosyst Eng.* 2012
34. Hong KK, Nielsen J. Metabolic engineering of *Saccharomyces cerevisiae*: a key cell factory platform for future biorefineries. *Cell Mol Life Sci.* 2012; 69:2671–2690. [PubMed: 22388689]
35. Brat D, Weber C, Lorenzen W, Bode HB, Boles E. Cytosolic relocalization and optimization of valine synthesis and catabolism enables increased isobutanol production with the yeast *Saccharomyces cerevisiae*. *Biotechnology for biofuels.* 2012; 5:65.10.1186/1754-6834-5-65 [PubMed: 22954227]
36. Urano, J., et al. US Patent Us 2011/0076733 A1. 2011.
37. Anthony, LC.; Huang, LL.; Ye, RW. US Patent US 201/0129886 A1. 2010.
38. Buelter, T.; Meinhold, P.; Smith, C.; Aristidou, A.; Dundon, CA.; Urano, J. WO Patent WO 2010/075504A2. 2010.
39. Szczebara FM, et al. Total biosynthesis of hydrocortisone from a simple carbon source in yeast. *Nat Biotechnol.* 2003; 21:143–149. [PubMed: 12514739]
40. Farhi M, et al. Harnessing yeast subcellular compartments for the production of plant terpenoids. *Metab Eng.* 2011; 13:474–481. [PubMed: 21601648]
41. Maarse AC, et al. Subunit IV of yeast cytochrome c oxidase: cloning and nucleotide sequencing of the gene and partial amino acid sequencing of the mature protein. *EMBO J.* 1984; 3:2831–2837. [PubMed: 6098449]
42. Larroy C, Pares X, Biosca JA. Characterization of a *Saccharomyces cerevisiae* NADP(H)-dependent alcohol dehydrogenase (ADHVII), a member of the cinnamyl alcohol dehydrogenase family. *Eur J Biochem.* 2002; 269:5738–5745. [PubMed: 12423374]
43. Dellomonaco C, Clomburg JM, Miller EN, Gonzalez R. Engineered reversal of the beta-oxidation cycle for the synthesis of fuels and chemicals. *Nature.* 2011; 476:355–359. [PubMed: 21832992]
44. Feldman, RMR., et al. US Patent US 2011/8017375 B2. 2011.
45. Wu S, et al. Redirection of cytosolic or plastidic isoprenoid precursors elevates terpene production in plants. *Nature biotechnology.* 2006; 24:1441–1447.
46. Christianson TW, Sikorski RS, Dante M, Shero JH, Hieter P. Multifunctional yeast high-copy-number shuttle vectors. *Gene.* 1992; 110:119–122. [PubMed: 1544568]
47. Sleight SC, Bartley BA, Lieviant JA, Sauro HM. In-Fusion BioBrick assembly and re-engineering. *Nucleic acids research.* 2010; 38:2624–2636. [PubMed: 20385581]
48. Blombach B, Eikmanns BJ. Current knowledge on isobutanol production with *Escherichia coli*, *Bacillus subtilis* and *Corynebacterium glutamicum*. *Bioeng Bugs.* 2011; 2:346–350. [PubMed: 22008938]
49. Gregg C, Kyryakov P, Titorenko VI. Purification of mitochondria from yeast cells. *J Vis Exp.* 200910.3791/1417



**Figure 1.** Isobutanol pathways. The upstream pathway (composed of ILV2, ILV5 and ILV3) is part of the valine biosynthetic pathway (red arrows), while the downstream pathway (composed of KDC and ADH) is the Ehrlich valine degradation pathway (green arrows). The  $\alpha$ -ketoisovalerate ( $\alpha$ -KIV) intermediate is interconverted to valine by BAT1 and BAT2. The upstream and downstream pathways are naturally separated between the mitochondria and cytoplasm, respectively (A). However, the pathway engineered via mitochondrial engineering targets the complete pathway to the mitochondrial compartment (B). Blue arrows depict transport across mitochondrial membranes.



**Figure 2.**

Isobutanol production by yeast engineered with mitochondrial and partly cytoplasmic isobutanol pathways. (A) Average isobutanol titers in 24-h high cell-density fermentations in minimal medium of the three highest producing colonies of each construct. The right panel summarizes the isobutanol titers obtained by the incremental addition of components of an isobutanol pathway targeted to mitochondria. (B) Isobutanol specific productivities vs isobutanol titers in 24-h high cell density fermentations of partial and complete isobutanol pathways containing only upstream *ILV* genes (yellow square); or also with their downstream enzymes targeted to mitochondria (filled markers) or cytoplasm (open markers). These include one of three  $\alpha$ -KDCs: Ll-kivd (red), Sc-kid1 (cyan) or Sc-aro10 (green); and either no ADH (diamond); or one of three ADHs: Sc-adh7 (circle), Ec-fucO (square), or Ll-adhA<sup>RE1</sup> (triangle); compared to empty plasmid (black full circle). Complete isobutanol pathways with their downstream enzymes targeted to the cytoplasm cluster with

pathways overexpressing only the *ILV* genes, and are shaded in grey. Partial 4-gene isobutanol pathways containing  $\alpha$ -KDCs targeted to mitochondria are shaded in red; and complete (5-gene) isobutanol pathways targeted to mitochondria are shaded in blue. (C) Time course of fermentations initiated at low cell densities in minimal medium. Strains with complete isobutanol pathways targeted to mitochondria are shown in continuous red (JAY153) and green (JAY161) lines; strains with the same downstream enzymes targeted to cytoplasm are shown in red (JAY166) and green (JAY174) dashed lines, respectively; strain JAY38 overexpressing only *ILV* genes is shown in yellow; and the background strain with empty plasmid (JAY2) is shown in black.

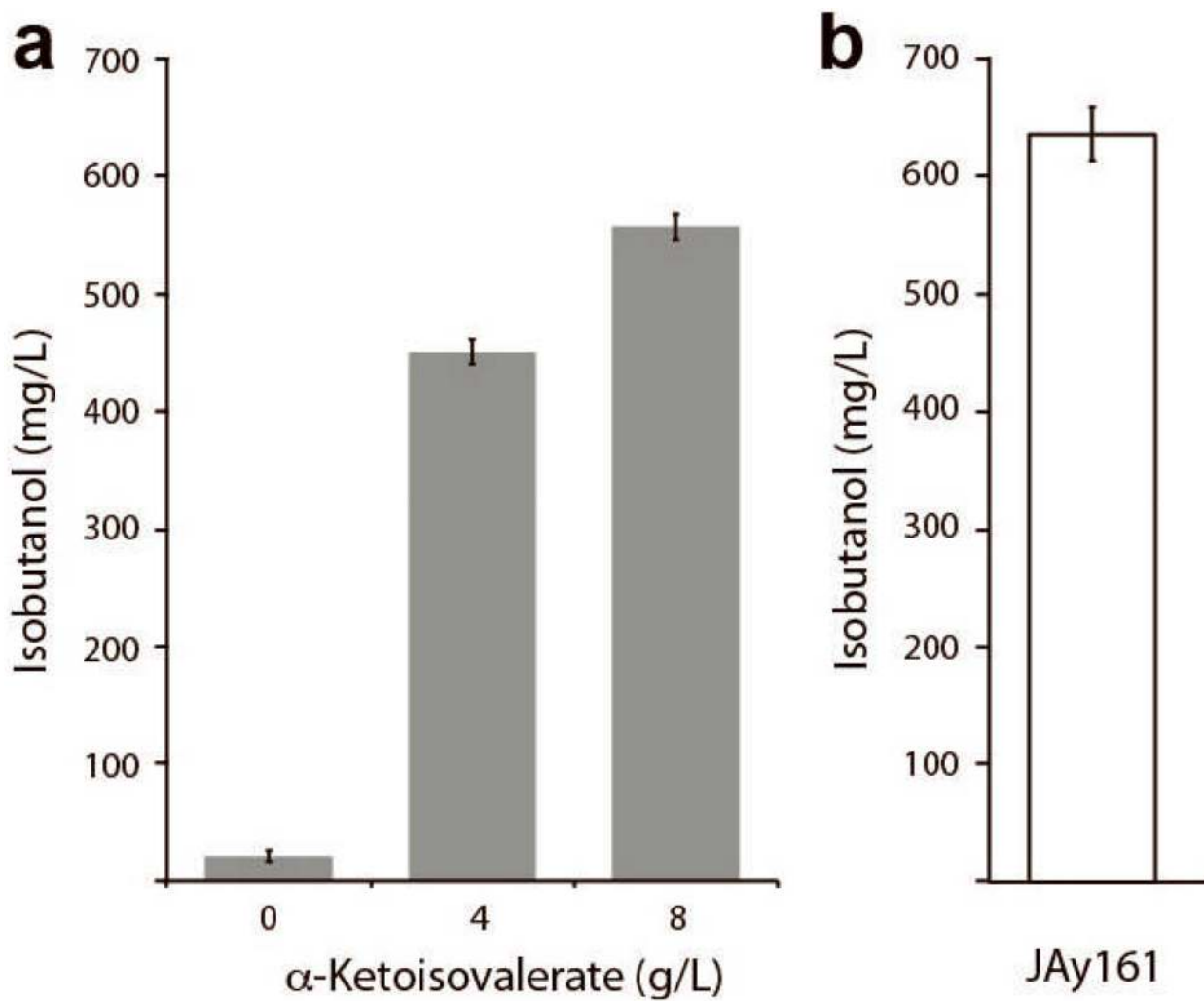


**Figure 3.** Cytoplasmic isobutanol production of a strain overexpressing Ll-kivd targeted to the cytoplasm, with or without addition of the  $\alpha$ -ketoisovalerate intermediate to the culture media (A); compared to isobutanol production of strain Jay161 (which has a mitochondrial pathway) without adding  $\alpha$ -ketoisovalerate (B).

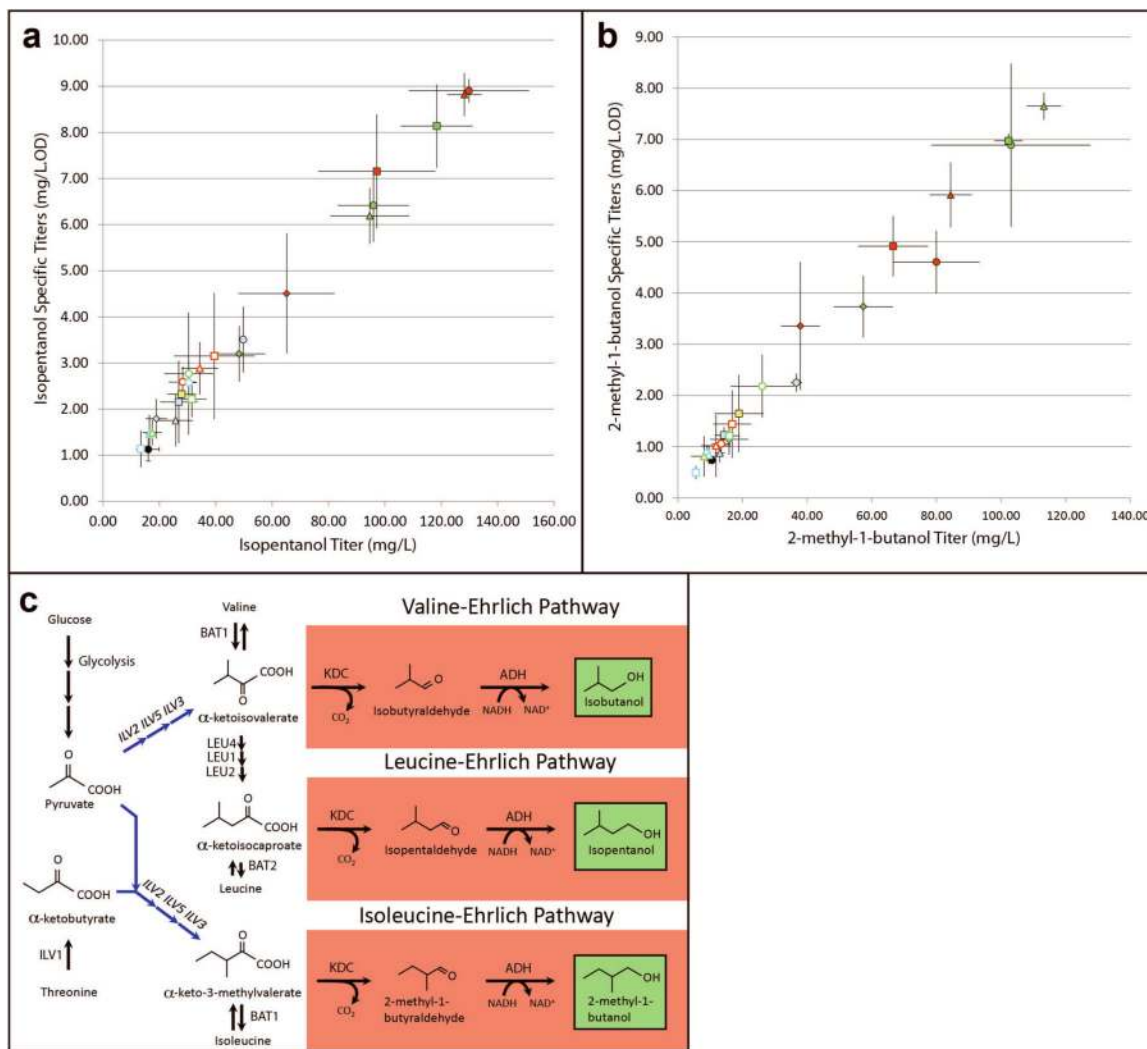


**Figure 4.**

Isopentanol and 2-methyl-1-butanol production. Specific productivity vs titer plots of isopentanol (A) and 2-methyl-1-butanol (B) obtained in 24-h high cell-density fermentations in minimal medium. The plots show the average titers and productivities of the three highest producing strains of each alcohol, for each construct. The constructs include partial and complete isobutanol pathways containing only upstream *ILV* genes (yellow square); or also with their downstream enzymes targeted to mitochondria (filled markers) or cytoplasm (open markers). These include one of three  $\alpha$ -KDCs: L1-kivd (red), Sc-kid1 (cyan) or Sc-aro10 (green); and either no ADH (diamond); or one of three ADHs: Sc-adh7 (circle), Ec-fucO (square), or L1-adhA<sup>RE1</sup> (triangle); compared to empty plasmid (black full circle). (C) The isobutanol, isopentanol and 2-methyl-1-butanol biosynthetic pathways have a significant overlap in their upstream pathways (blue arrows); and identical downstream, Ehrlich degradation pathways (red boxes).

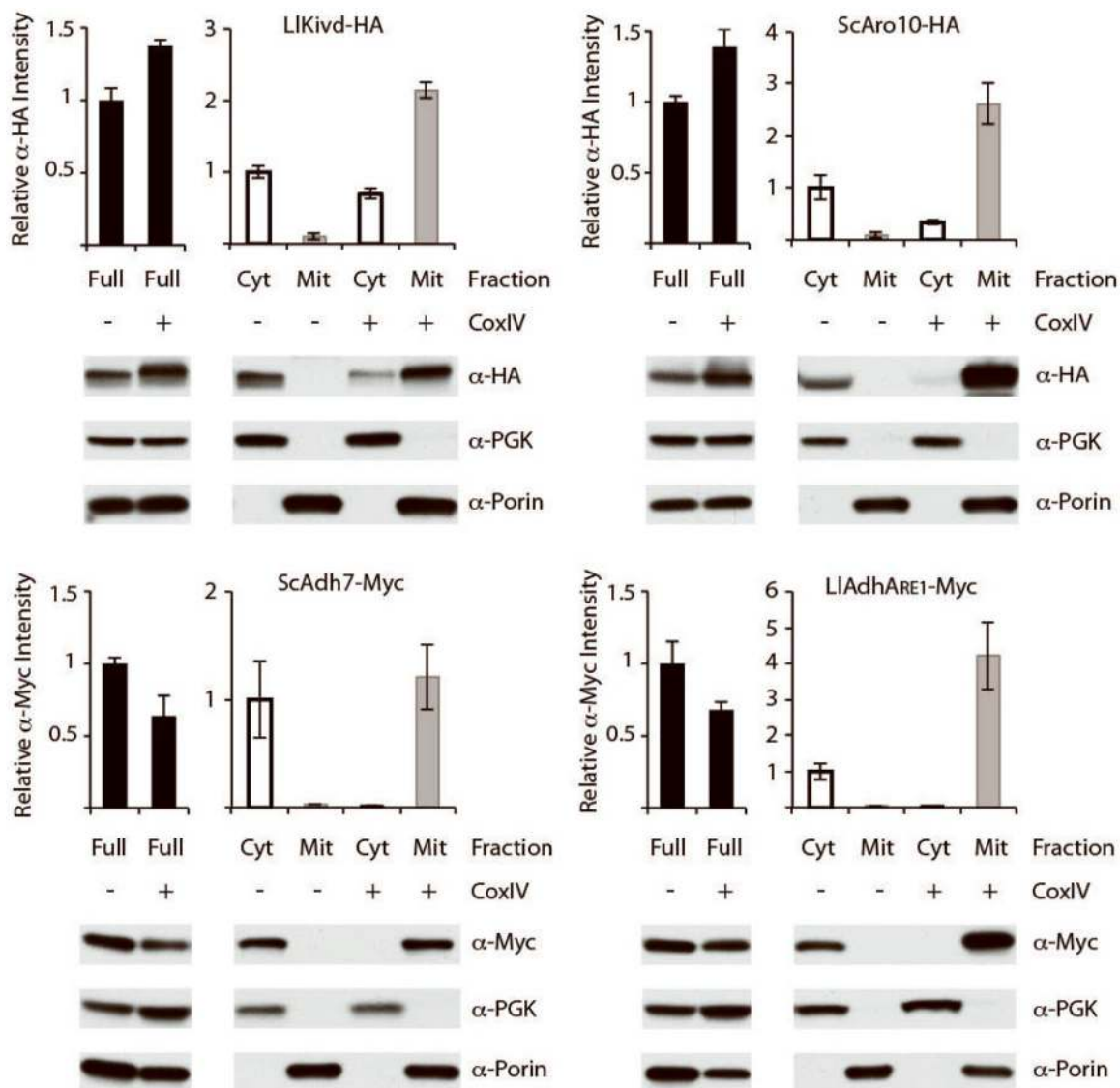


**Figure 5.** Subcellular distribution of  $\alpha$ -KDCs and ADHs fused to -HA or -Myc tags respectively, and targeted to cytoplasm (CoxIV -) or mitochondria (CoxIV+). Gels were loaded with 20  $\mu$ g of total protein from cytoplasmic (Cyt) or mitochondrial (Mit) fractions; or equal amounts of full cells (Full). Densitometry measurements of cytoplasmic and mitochondrial fractions are shown in histograms of relative intensities normalized to signals of enzymes targeted to the cytoplasm. Densitometry measurements of full cell samples (Full) are shown in separate histograms of relative intensities normalized to signals from strains with enzymes targeted to the cytoplasm. As controls, the distributions of PGK and porin, which are specific markers for the cytoplasmic and mitochondrial fractions respectively, were determined on the same blots.

**Table 1**

Summary of the highest titers, yields, and productivities achieved for isobutanol, isopentanol and 2-methyl-1-butanol with JAy161.

| <b>JAy161</b>         | <b>Isobutanol*</b> | <b>Isopentanol<sup>#</sup></b> | <b>2-methyl-1-butanol<sup>#</sup></b> | <b>Total Fusel Alcohols</b> |
|-----------------------|--------------------|--------------------------------|---------------------------------------|-----------------------------|
| Titer (mg/L)          | 635 ± 23           | 95 ± 12                        | 118 ± 28                              | 850 ± 60                    |
| Yield (mg/g.glucose)  | 6.7 ± 0.2          | 1.0 ± 0.1                      | 1.2 ± 0.2                             | 9.0 ± 0.5                   |
| Productivity (mg/L.h) | 20.5 ± 1.2         | 4.0 ± 0.6                      | 4.7 ± 0.2                             | 29 ± 2                      |

\* The highest isobutanol production levels previously reported<sup>35</sup> are: titer 630 ± 14 mg/L; yield 14.9 ± 0.6mg/g.glucose; and productivity (calculated) 6.6 ± 0.1 mg/L.h. These values correspond to fermentations in which valine was excluded from the media, as this nutrient inhibits isobutanol production of their strains.

<sup>#</sup> Overproduction of isopentanol or 2-methyl-1-butanol in engineered yeast has not been previously reported.